

# Radical-initiated copolymers of *N*-vinyl pyrrolidone and *N*-acryloxy succinimide: kinetic and microstructure studies

Marie-Noëlle Erout, Abdelhamid Elaïssari and Christian Pichot\*  
*Unité mixte CNRS-BioMérieux, ENSL, 46 allée d'Italie, 69364 Lyon, France*

and Marie-France Llauro  
*LMOPS/CNRS, BP 24, 69390 Vernaison, France*  
(Received 21 September 1994; revised 11 July 1995)

Kinetics of solution (co)polymerization of *N*-vinyl pyrrolidone (NVP, or V) and *N*-acryloxy succinimide (NAS, or A) have been investigated at 60°C in *N,N*-dimethylformamide with 4,4'-azobis(4-cyanopentanoic acid) as initiator. First, the  $k_p/\sqrt{k_t}$  value for homopolymerization of A monomer was estimated as  $0.87 \text{ l}^{0.5} \text{ mol}^{-0.5} \text{ s}^{-0.5}$ . The comonomer feed composition was observed to have a strong effect on the overall copolymerization rate. Reactivity ratios of the binary system were determined to be  $r_{\text{NAS}} = 0.27 \pm 0.04$  and  $r_{\text{NVP}} = 0.01 \pm 0.01$ , indicating a strong alternating tendency in the formed copolymer. Copolymers were then characterized as regards to composition (by ultraviolet spectrophotometry) and monomer sequence distribution (by  $^{13}\text{C}$  nuclear magnetic resonance spectroscopy). The presence of a small fraction of VVA triads was clearly evidenced which was not expected from simulation based on a terminal kinetic model; the occurrence of a more complex model has been discussed.

(Keywords: radical copolymers; *N*-vinyl pyrrolidone; *N*-acryloxy succinimide; alternated microstructure)

## INTRODUCTION

The polymerization and chemistry of activated esters have been developed in recent years to provide a versatile method for preparing functional polymers. This route is simple and suitable for the synthesis of numerous polymers which can be applied in many fields (such as chemistry, engineering, biotechnology and medicine)<sup>1</sup>.

Copolymers with activated esters of unsaturated acids have been found quite valuable for reacting with biomolecules containing primary amine groups. For example, copolymers of *N*-isopropyl acrylamide and *N*-acryloxy succinimide have been used for the immobilization of monoclonal antibodies<sup>2,3</sup>, immunoglobulins (IgG)<sup>4</sup> and enzymes<sup>5</sup>. However, a few studies have been devoted to such binary copolymerizations involving unsaturated acids as well as their molecular and physico-chemical properties.

The case of *N*-vinyl pyrrolidone as comonomer is interesting since it can provide some outstanding features such as hydrophilicity and biocompatibility. In a recent paper, Nazarova *et al.*<sup>6</sup> reported a short study on the kinetics of free-radical copolymerization of *N*-vinyl pyrrolidone with different *N*-hydroxy phthalimide and *N*-hydroxy succinimide esters of acrylic, methacrylic and crotonic acids. An important result was that in most of the binary systems both reactivity ratios were near zero,

which indicated that a strong alternating tendency had been operating during copolymerization.

As part of a programme to prepare well-characterized functional copolymers to be used further as hydrophilic supports in biological applications, a preliminary study has been directed on the synthesis of *N*-vinyl pyrrolidone (NVP) and *N*-acryloxy succinimide (NAS) copolymers. Since the radical-initiated copolymerization involving NVP is usually characterized by a value of  $r_{\text{NVP}}$  near 0, it was expected that copolymer chains with a broad range of compositions would be formed, except if such systems exhibit an azeotropic composition or if low-conversion conditions could be selected. Hence, the two main objectives of this work were: (1) to conduct a detailed kinetic analysis allowing the determination of several pertinent parameters, especially the reactivity ratios of the binary system; and (2) to characterize the ultimate copolymers in terms of composition and microstructure.

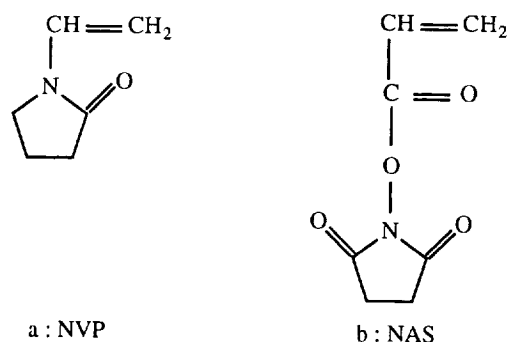
## EXPERIMENTAL

### Materials

*N*-Vinyl pyrrolidone (NVP; 99% from Kodak, Rochester, NY, USA) was purified by distillation under reduced pressure; *N*-acryloxy succinimide (NAS; 99% from Kodak) was used as-received or recrystallized in ethyl acetate/pentane mixture. The following formulae

\* To whom correspondence should be addressed

describe the chemical structure of the two monomers:



4,4'-Azobis(4-cyanopentanoic acid) (kindly provided by Wako Chemicals, Neuss, Germany) was the initiator and used as-received. *N,N*-Dimethylformamide (DMF, from Aldrich, Milwaukee, WI, USA) was used as solvent.

#### Solution copolymerization procedure

Polymerization experiments were performed in a three-necked round-bottomed flask equipped with a magnetic stirrer and azote inlet. The reaction vessel was loaded with the solvent (DMF) and the comonomer mixture at an overall concentration of  $0.5 \text{ mol l}^{-1}$ , and then purged with nitrogen for 2 h. The temperature was raised to  $60^\circ\text{C}$  using a thermostatted oil bath and, finally, the initiator mixture dissolved in the remainder of the solvent was added to the reaction mixture. The copolymerization was carried out under a nitrogen atmosphere.

#### Kinetic studies

Samples were withdrawn at different reaction times and placed in vials containing traces of hydroquinone as an inhibitor to stop the polymerization, then stored at  $-20^\circ\text{C}$ .

Monomer consumption was followed by gas chromatography (g.c.) analysis. Separation was performed with a DELSI equipment (DI)  $200^\circ\text{C}$  on an SE 30 (100% methyl silicone) column (1.5 m length) at  $175^\circ\text{C}$  and using flame ionization detection; in the case of the NVP homopolymerization kinetics, a glass column (10% Carbowax 20M onto Chromosorb WAW 80/10 mesh, 2 m length) was used. In all cases, the amount of residual monomer was calculated from monomer and solvent (internal standard) peak areas according to the following equation:

$$[M]_t = \left[ \frac{(S_M)_{t=0}}{(S_{DMF})_{t=0}} \right] / \left[ \frac{(S_M)_t}{(S_{DMF})_t} \right] [M]_{t=0} \quad (1)$$

where  $(S_M)_{t=0}$ ,  $(S_{DMF})_{t=0}$  are the peak areas corresponding to initial concentrations of monomer and solvent, respectively;  $(S_M)_t$  is the residual monomer peak area after a polymerization time  $t$ .

From the initial slopes, initial copolymerization rates  $R_{NVP,0}$  and  $R_{NAS,0}$  for *N*-vinyl pyrrolidone and *N*-acryloxy succinimide, respectively, were determined, from which the average initial copolymer composition

was calculated according to the following relationship:

$$F_{NAS,0} = \frac{R_{NVP,0}}{R_{NVP,0} + R_{NAS,0}} = \frac{\frac{d[NAS]}{dt}}{\frac{d[NAS]}{dt} + \frac{d[NVP]}{dt}} \quad (2)$$

For NAS-poor comonomer feed compositions, due to the high NVP consumption rate, kinetics were followed by direct  $^1\text{H}$  nuclear magnetic resonance (n.m.r.) analysis of the reaction mixture.

#### Copolymer characterization

**Average copolymer composition.** For all experiments, due to strong reactivity of the monomers, high conversions (70–80%) were generally achieved within a short time. Copolymers were then precipitated with ethylic ether, filtered, washed several times with the same solvent and finally dried under vacuum.

Three spectroscopic methods were used for determining the copolymer composition: ultraviolet (u.v.) spectrophotometry, Fourier transform infra-red (FT i.r.) spectroscopy and  $^1\text{H}$  n.m.r. spectroscopy. The former was found to be more appropriate for getting reliable and reproducible data. The principle was based on the analysis of the absorption band of the hydroxy succinimide anion resulting from the aminolysis of  $\text{NH}_4\text{OH}$ . Dimethylformamide was added to favour the solubility of all copolymers and a large excess of  $\text{NH}_4\text{OH}$  was used to obtain complete hydrolysis of the esters. Therefore, the molar extinction coefficient ( $\epsilon$ ) was  $7100 \text{ l mol}^{-1} \text{ cm}^{-1}$  instead of  $9700 \text{ l mol}^{-1} \text{ cm}^{-1}$  in pure basic water.

**Copolymer microstructure.** High resolution  $^{13}\text{C}$  n.m.r. spectroscopy was carried out with a Bruker AC200 equipment working at 50.3 MHz for  $^{13}\text{C}$ . Deuterated DMF (d7-DMF) was used as solvent and dioxane or tetramethylsilane (TMS) as internal standard.

## RESULTS AND DISCUSSION

#### Kinetic studies

**Homopolymerization of *N*-acryloxy succinimide.** Since the behaviour of NAS in radical-initiated polymerization has not been reported previously, conversion *versus* time data were used to calculate values of  $k_p/\sqrt{k_t}$ . According to the well-known relationship giving the variation of monomer concentration as a function of time taking into account the initiator decomposition,

$$-\frac{d[M]}{dt} = k_p \frac{\sqrt{fk_d[I]_0}}{\sqrt{k_t}} [M] \exp\left(\frac{-k_d t}{2}\right) \quad (3)$$

where  $k_p$ ,  $k_t$ ,  $k_d$  are absolute rate constants for propagation, termination and initiator decomposition, respectively;  $f$  is the initiator efficiency;  $[M]_0$  is the initial monomer concentration;  $[M]$  is the residual monomer concentration; and  $[I]_0$  is the initiator concentration at  $t = 0$ .

Integration of equation (3) yields:

$$-\ln\left(\frac{[M]_t}{[M]_0}\right) = \frac{2k_p\sqrt{f[I]_0}}{\sqrt{k_t k_d}} \left[1 - \exp\left(\frac{-k_d t}{2}\right)\right] \quad (4)$$

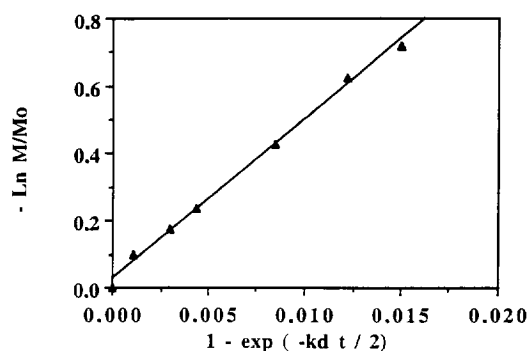


**Figure 1** Semi-logarithmic variation of the NAS monomer consumption versus the decomposition rate of the initiator [according to equation (4)]

$k_p/\sqrt{k_t}$  was determined by calculating the slope of  $-\ln([M]_t/[M]_0)$  as a function of  $[1 - \exp(-k_d t/2)]$  for NAS homopolymerization (Figure 1), with  $k_d = 1.05 \times 10^{-5} \text{ s}^{-1}$  at  $60^\circ\text{C}$  in DMF<sup>7</sup>, which is close to the value reported<sup>8</sup> for azobisisobutyronitrile ( $0.98 \times 10^{-5} \text{ s}^{-1}$ ) in toluene at  $60^\circ\text{C}$ , and with  $f = 0.5$ <sup>9</sup>. This procedure gives a value for  $k_p/\sqrt{k_t}$  of  $0.881^{0.5} \text{ mol}^{-0.5} \text{ s}^{-0.5}$  for NAS homopolymerization; the value for NVP homopolymerization has recently been reported<sup>8</sup> to be  $0.241^{0.5} \text{ mol}^{-0.5} \text{ s}^{-0.5}$ .

The value obtained for the *N*-acryloxy succinimide is slightly higher than those reported for acrylates with short alkyl esters (for example, 0.68 and  $0.671^{0.5} \text{ mol}^{-0.5} \text{ s}^{-0.5}$  for methyl and ethyl acrylate<sup>10</sup>, respectively, at the same reaction temperature). As similarly suggested

**Table 1** Radical-initiated<sup>a</sup> copolymerization of NAS with NVP. Effect of the initial monomer feed composition ( $f_{\text{NAS},0}$ ) on the individual ( $V_{\text{NVP}}$  and  $V_{\text{NAS}}$ )<sup>b</sup> and overall ( $R_{p,0}$ ) rates of polymerization

	$f_{\text{NAS},0}$	$[\text{NVP}]_0^c$ ( $\text{mol l}^{-1}$ )	$[\text{NAS}]_0^c$ ( $\text{mol l}^{-1}$ )	$V_{\text{NVP}} \times 10^4$ ( $\text{s}^{-1}$ )	$V_{\text{NAS}} \times 10^4$ ( $\text{s}^{-1}$ )	$R_{p,0} \times 10^5$ ( $\text{mol l}^{-1} \text{ s}^{-1}$ )
PNVP		0.500				2.00
COPO10						
n.m.r.	0.100	0.450	0.050	3.20	28.00	28.40
COPO20						
g.c.	0.200	0.400	0.100	3.20	13.40	26.20
n.m.r.	0.200	0.400	0.100	2.90	13.80	25.40
COPO35	0.350	0.325	0.179	4.05	10.70	32.30
COPO48	0.480	0.260	0.240	3.18	4.12	18.10
COPO64	0.640	0.184	0.328	3.05	2.75	14.70
COPO74	0.740	0.133	0.370	4.18	2.53	14.90
PNAS	1.000		0.500			6.85

<sup>a</sup> Initial concentration of initiator  $[\text{I}]_0 = 5 \times 10^{-3} \text{ mol l}^{-1}$  for each copolymerization

<sup>b</sup>  $V_{\text{NVP}} = \frac{1}{[\text{NVP}]_0} \frac{d[\text{NVP}]}{dt}$ ;  $V_{\text{NAS}} = \frac{1}{[\text{NAS}]_0} \frac{d[\text{NAS}]}{dt}$

<sup>c</sup>  $[\text{NVP}]_0$  and  $[\text{NAS}]_0$  are initial concentrations of NVP and NAS, respectively

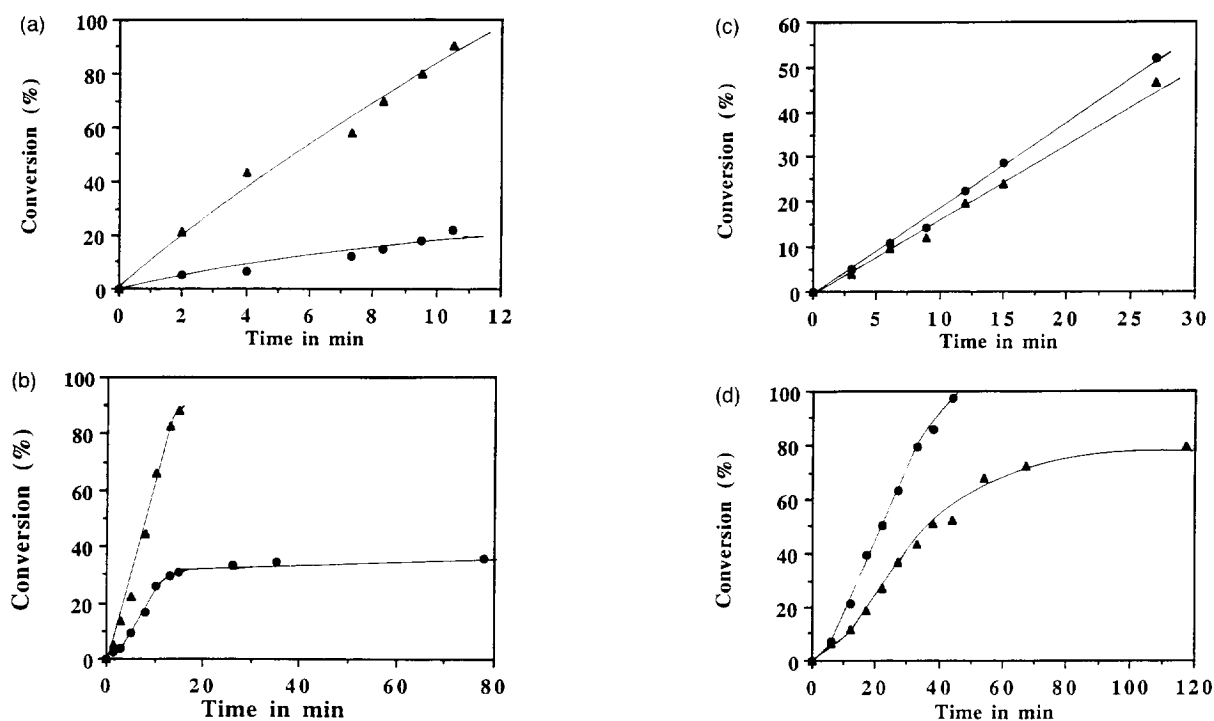


**Figure 2** Individual monomer consumption versus time for various copolymerizations of NVP with NAS in DMF solution: (a) COPO20, (b) COPO35, (c) COPO64, (d) COPO74. ●, NVP conversion; ▲, NAS conversion

by Abajo *et al.*<sup>11</sup> for *N*-(2-acryloxy ethyl) phthalimide, such a result can be explained by a decrease of the termination rate constant caused by the stiffness conferred by the succinimide side group to the growing radical.

**NVP–NAS copolymerization.** Kinetic studies of the NAS–NVP radical-initiated copolymerization were conducted for five different initial comonomer feed compositions. The consumption of each comonomer was followed accurately by g.c. analysis, allowing extrapolation to zero conversion and, therefore, a rapid and easy estimation of each initial conversion rate. All experimental conditions and kinetic data are compiled in *Table 1*.

Individual monomer consumptions *versus* time are reported in *Figures 2a–d* for copolymerizations containing 20, 35, 64 and 74 mol% NAS in the feed, respectively. Three main features may be pointed out: (1) the initial consumption rates are extremely rapid for both monomers; (2) the consumption rate for NVP decreases drastically when NAS monomer is depleted, especially in the NAS-rich composition domain; (3) above 60 mol% NAS, an inversion clearly appears in the consumption rates of both monomers, suggesting the existence of an azeotropic composition.

The overall initial rate of copolymerization was found to be much higher than the NVP and NAS homopolymerization rates (as deduced from experimental data reported in *Table 1*). As illustrated in *Figure 3*, a maximum value is clearly in evidence for an initial monomer feed composition around 30 mol% NAS. This effect was also reported by Nazarova *et al.*<sup>6</sup> and will be discussed in more detail later.

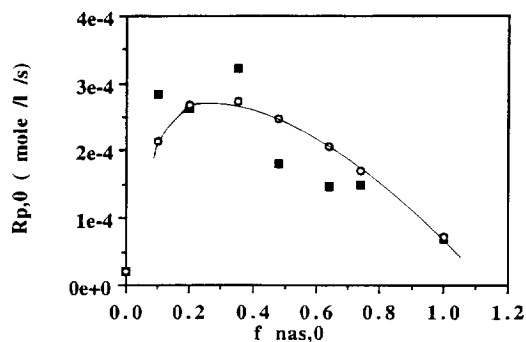


**Figure 3** Initial copolymerization rate ( $R_{p,0}$ ) *versus* NAS content ( $f_{\text{NAS},0}$ ) in the monomer mixture (molar fraction): ■, experimental data; ○, simulated data

**Reactivity ratios.** Reactivity ratios were determined using the conventional graphical methods of Fineman–Ross (FR)<sup>12</sup> and Kelen–Tüdös (KT)<sup>13</sup>, and a non-linear method of Tidwell–Mortimer (TM)<sup>14</sup>. From the data reported in *Table 2*, the average values for the reactivity ratios are  $r_{\text{NAS}} = 0.27 \pm 0.04$  and  $r_{\text{NVP}} = 0 \pm 0.08$ , indicating good precision for  $r_{\text{NAS}}$  and poor precision for  $r_{\text{NVP}}$  (since the negative values appearing from the extrapolation do not have any physical meaning).

Such a value was indeed expected from the work of Nazarova *et al.*<sup>6</sup> as well as from a review of literature data for reactivity ratios for many binary systems containing NVP and various acrylates (see *Table 3*). It is clear, particularly for activated esters of unsaturated acids, that  $r_{\text{NVP}}$  is always near 0. In addition, since in most cases ( $r_1 \times r_2$ ) tends towards zero, it is obvious that strong cross-propagation occurs during the copolymerization of such systems, as in the case of NVP–NAS, with a high alternance tendency in the resulting copolymer chains. However, our value for NAS appears to be significantly different from that reported by Nazarova *et al.*<sup>6</sup>.

This alternance tendency is also confirmed using the so-called square diagram (*Figure 4*), which reports the instantaneous copolymer composition ( $F_1$ ) *versus* the initial comonomer feed composition ( $f_1$ ). It is worthy to note that  $F_{\text{NAS}}$  almost reaches 50 mol% regardless of  $f_{\text{NAS}}$  up to 70 mol%, precluding the preparation of

**Table 3** Literature reactivity ratios for NVP (2)/acrylate (1) binary systems

	Reactivity ratios	Ref.
<i>N</i> -Acryloxy succinimide	$r_1 = 0.27 \pm 0.04$ $r_2 = 0 \pm 0.08$	This work
	$r_1 = 0.045 \pm 0.045$ $r_2 = 0.045 \pm 0.045$	6
<i>N</i> -Acryloxy phthalimide	$r_1 = 0.033 \pm 0.027$ $r_2 = 0.018 \pm 0.018$	6
	$r_1 = 2.28 \pm 0.32$ $r_2 = 0.025 \pm 0.016$	6
2,4,5-Trichlorophenyl acrylate	$r_1 = 0.16 \pm 0.01$ $r_2 = 0.01 \pm 0.02$	15
2-Hydroxymethyl methacrylate	$r_1 = 4.35 \pm 0.04$ $r_2 = 0.06 \pm 0.10$	15
Glycidyl methacrylate	$r_1 = 3.84 \pm 0.40$ $r_2 = 0.026 \pm 0.070$	16
	$r_1 = 4.32 \pm 0.20$ $r_2 = 0.0075 \pm 0.0075$	17

**Table 2** Reactivity ratios for free-radical copolymerization of NVP (2) with NAS (1)

Copolymerization experiments	FR <sup>a</sup>	KT <sup>b</sup>	TM
COPO 10/20/48/64/74	$r_1 = 0.250 \pm 0.05$ $r_2 = 0.008 \pm 0.1$		
COPO 10/20/48/64/74		$r_1 = 0.28 \pm 0.03$ $r_2 = 0.02 \pm 0.08$	
COPO 10/20/35/48/64/74			$r_1 = 0.28 \pm 0.03$ $r_2 = 0 \pm 0.1$

<sup>a</sup> Correlation coefficient = 0.98

<sup>b</sup> Correlation coefficient = 0.94

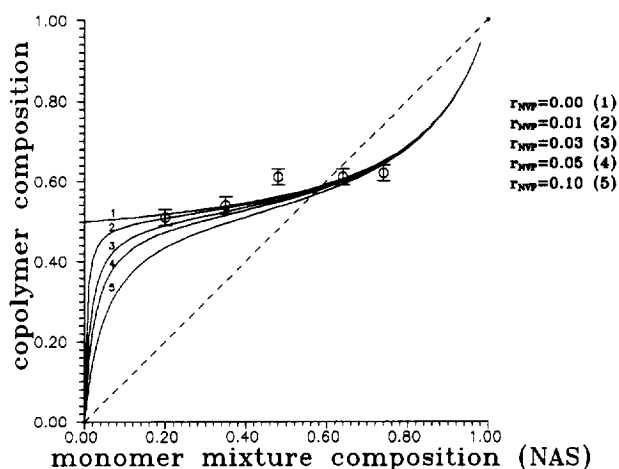


**Figure 4** Square diagram of the instantaneous copolymer composition ( $F_{\text{NAS},0}$ ) versus the comonomer feed composition ( $f_{\text{NAS},0}$ ). Experimental data and calculated curves for  $r_{\text{NAS}} = 0.27$  and  $r_{\text{NVP}} = 0.00$  (1), 0.01 (2), 0.03 (3), 0.05 (4), 0.10 (5)

**Table 4** Instantaneous copolymer composition  $F_{\text{NAS},0}$  (derived from gas chromatography or n.m.r. (\*) analysis of the reaction mixture) versus comonomer feed composition ( $f_{\text{NAS},0}$ ) in solution copolymerization

$f_{\text{NAS},0}$	$F_{\text{NAS},0}$ (experimental data)	$F_{\text{NAS},0}$ (theoretical values)	
		$r_{\text{NAS}} = 0.27$ $r_{\text{NVP}} = 0.00$	$r_{\text{NAS}} = 0.27$ $r_{\text{NVP}} = 0.01$
0.10	0.50 (*)	0.51	0.48
0.20	0.51	0.52	0.51
	0.54 (*)		
0.35	0.58	0.54	0.53
0.48	0.54	0.56	0.56
0.64	0.61	0.60	0.60
0.74	0.63	0.65	0.65

**Table 5** Influence of the monomer feed composition on the factor  $\Phi$

Experiment	$f_{\text{NAS},0}$	$\Phi$
COPO10	0.10	0.15
COPO20	0.20	1.1–1.3
COPO35	0.35	0.05
COPO48	0.48	5.3
COPO64	0.64	9.1
COPO74	0.74	4.9

homogeneous copolymers, except if the azeotropic composition (around 59 mol% NAS) can be used.

As illustrated in the two last columns of Table 4, comparison of experimental with theoretical data ( $F_{\text{NAS},0}$  versus  $f_{\text{NAS},0}$ ) shows good agreement except for COPO35 ( $f_{\text{NAS},0} = 0.35$ ), for which the initial instantaneous composition is slightly higher than the calculated value.

As already stated, good precision was exhibited for  $r_{\text{NAS}}$ , whereas  $r_{\text{NVP}}$  was poorly determined. To evaluate the latter more accurately, a simulation of the  $F_{\text{NAS},0}$  versus  $f_{\text{NAS},0}$  curve was performed keeping  $r_{\text{NAS}}$  constant and changing  $r_{\text{NVP}}$  in a range of reasonable values (i.e. between 0.0 and 0.1). This is well illustrated in the square diagram reported in Figure 4, showing that the best fit with experimental data (especially for NVP-rich comonomer mixtures) is observed when the selected  $r_{\text{NVP}}$

value is near 0.01. This value was therefore used in further copolymerization modelling.

Now, the knowledge of these various kinetic parameters allows one to work out the influence of the comonomer feed composition on the overall initial rate of copolymerization. Such behaviour can be simulated using the following copolymerization rate equation:

$$R_p = \frac{r_V[V]^2 + 2[V][A] + r_A[A]^2}{\sqrt{r_V^2\delta_V^2[V]^2 + 2\Phi r_V r_A[V][A]\delta_V\delta_A + r_A^2\delta_A^2[A]^2}} \sqrt{R_i} \quad (5)$$

where V and A refer to *N*-vinyl pyrrolidone and *N*-acryloxy succinimide, respectively; and  $\delta_V$  and  $\delta_A$  parameters are equal to  $\sqrt{2\sqrt{k_{tAV}}/k_p}$  for V and A homopolymerization, respectively. Since all the kinetic parameters of this equation have been determined,  $R_p$  can be calculated, assuming that  $\Phi$ , which represents the ratio of half the cross-termination rate constant to the geometric mean of the rate constants for self-termination of like radicals (i.e.  $k_{tAV}/2\sqrt{k_{tAA}k_{tVV}}$ ), is equal to 1. The data are reported in Figure 3 together with the experimental ones. Two important observations can be made: (1) the strong increase in the copolymerization rate compared with both homopolymerization rates is confirmed, with a maximum value near 30 mol% NAS; (2) it seems that the agreement with experimental data deviates drastically in the intermediate composition range.

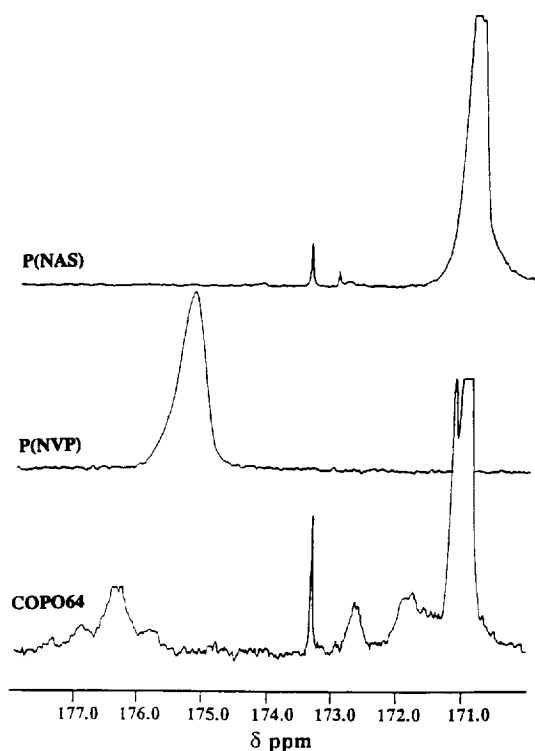
Such an effect can be tentatively explained in remembering that the copolymerization rate is dependent upon both propagation and termination rate constants; the large increase observed in  $R_{p,0}$  would indicate the dominance of the cross-propagation rate, which is indeed the main kinetic event in a copolymerization where the alternance tendency is very high. Furthermore, the poor agreement between experimental and theoretical data in the intermediate composition range would suggest the inadequacy of the assumption concerning the  $\Phi$  value for calculating  $R_{p,0}$ . This can be accounted for by back-determining the  $\Phi$  factor using the actual overall copolymerization rate; from the data collected in Table 5, it is obvious that  $\Phi$  is dependent on monomer feed composition, the largest values being obtained for experiments COPO48 and COPO64 ( $\Phi = 5.3$  and 9.1, respectively).

#### Characterization of NVP–NAS copolymers

**Average copolymer composition.** Several of the NAS–NVP copolymers were precipitated at given conversions and, after drying, their composition was obtained by u.v. spectrophotometry, since this technique was found to be the more appropriate. Results are reported in Table 6 in the case of four different copolymers. Considering the precision of the method, there is relatively fair agreement between experimental and theoretical data, taking into account the actual reactivity ratios and degree of conversion. Concerning sample COPO64, the agreement is quite satisfactory and the overall composition versus conversion (except for the high-conversion sample) is nearly constant, corroborating that the selected initial monomer feed composition was not far from the expected azeotropic one.

**Table 6** NAS–NVP solution copolymers. Comparison of experimental and theoretical average compositions

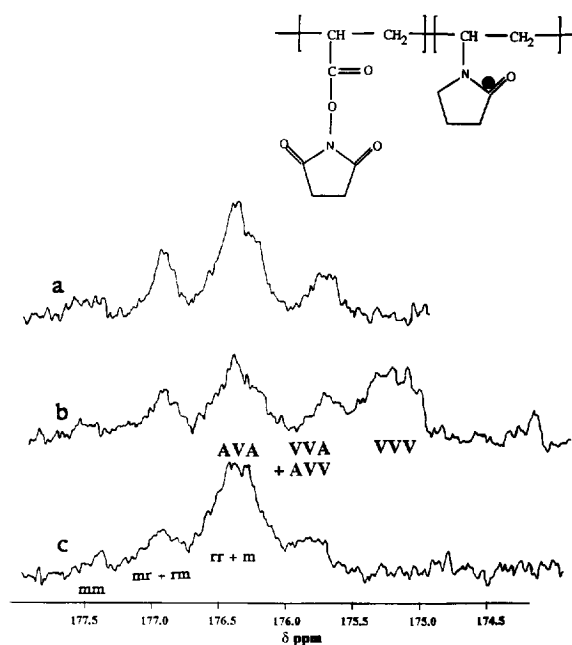
Sample	$f_{\text{NAS},0}$	Conversion (wt%)	$F_{\text{NAS},\text{exp}}$	$F_{\text{NAS},\text{theo}}$ ( $r_{\text{NAS}} = 0.27$ , $r_{\text{NVP}} = 0.01$ )
COPO10	0.10	10	0.50	0.48
		30	0.37	0.33
COPO20	0.20	50	0.50	0.40
COPO48	0.48	90	0.60	0.53
COPO64	0.64	7	0.63	0.60
		13	0.57	0.60
		35	0.57	0.60
		50	0.57	0.60
		90	0.48	0.60


**Figure 5**  $^{13}\text{C}$  n.m.r. spectra (50.3 MHz) of both homopolymers (PNVP and PNAS) and a copolymer (64 mol% NAS) in  $d_7$ -DMF

**Monomer sequence distribution.** The microstructure of these copolymers (and especially their monomer sequence distribution) was thoroughly investigated for two main reasons:

- (1) to compare the experimental monomer sequence distribution (provided a compositional effect can be identified in such copolymers, which was indeed shown by Nazarova *et al.*<sup>6</sup>) with the theoretical one deduced from reactivity ratios and numerical simulation based on first-order Markov statistics; and
- (2) to obtain a more precise description of these copolymers with a view to using them further for covalent immobilization of biomolecules.

Generally, the monomer sequence distribution in an A/B copolymer can be studied by n.m.r. provided a compositional effect (for example, a difference in  $\text{CH(A)}$  chemical shift between  $\text{AAA}$ ,  $\text{AAB}$  and  $\text{BAB}$  triads) is high enough compared with the configurational effect<sup>18</sup>.


**Figure 6**  $^{13}\text{C}$  n.m.r. spectra (50.3 MHz) of copolymers: (a) COPO10, 10% conversion; (b) COPO10, 30% conversion; (c) COPO64, 80% conversion

First, the various carbon resonance structures of both homopolymers and a 64 mol% NAS (A) copolymer were identified so as to detect and discriminate configurational (cf) and compositional effects (as shown in *Figure 5*). Splitting observed on the carbonyl carbon in the NAS homopolymer (PNAS) is ascribed to a tacticity effect ( $\Delta\delta_{\text{cf}} = 2.25$  ppm), but no such effect is observed in the case of the NVP homopolymer (PNVP). When considering the copolymer, it seems obvious from the large splitting of the NVP (V) carbonyl resonance that a compositional effect does interfere with probably a simultaneous co-configurational effect brought about by VA dyads (*Figure 5*).

A more detailed analysis was performed so as to assign the various triad sequences. If only a compositional effect is considered, three peaks should have been observed corresponding to AVA, AVV and VVV; since the configurational effect is due only to AV dyads, five peaks are expected (*mm*, *rm* and *rr* of AVA, *r* and *m* of AVV). The reported copolymer spectrum (*Figure 5*) seems to exhibit four peaks (between 175.5 and 177.5 ppm) with the absence of any VVV triad (that is to say, no V sequence longer than two units). This is not surprising for this copolymer, which corresponds to the azeotropic composition: a simulation of the triad distribution showed only the presence of AVA and AVV triads. At this composition, the copolymer composition is homogeneous throughout the conversion, and the distribution of the monomer units along the polymer chain is invariant, too.

For a better and unambiguous assignment of the various expected triads, another copolymer was considered (10 mol% A) in which the presence of VVV triads could be identified. Simulation of such a copolymerization indeed showed that VVV triads are expected at relatively low conversion (above 20%) with a drastic variation of both A- and V-centred triad distributions. In *Figure 6c* is displayed the enlarged carbonyl resonance

region related to the A unit and corresponding to the azeotropic composition (64 mol% A) at 85% conversion. In comparison with the spectrum of PNVP, the structure located at higher field for the higher conversion 10 mol% NAS (A) copolymer around 175.25 ppm (Figure 6b) was assigned to the VVV triad ( $\delta = 175.20$  ppm in the PNVP).

In order to identify the other peaks, it was assumed that, due to steric hindrance factors, the racemic configuration was the most probable dyad configuration in the copolymer chain, as is usually observed in radical polymerization<sup>19</sup>. Hence, in the case of AVA triads, the three different configurations *mm*, *mr* (or *rm*) and *rr* are located consecutively from lower to higher fields at 177.5, 176.9 and 176.4 ppm, respectively. In such a way,  $\Delta\delta_{cf}$  being around 0.5 ppm, the peak at 175.8 ppm is attributed to the most probable AVV triad comprising a racemic AV dyad, the meso AV diad being probably overlapped under the syndiotactic (*rr*) AVA triad. This assignment was found to be relevant for the spectra of the other copolymers (see, for example, the case of a 20 mol% A copolymer).

Finally, a quantitative analysis of the V-centred triad distribution was performed allowing us to corroborate the above-described assignment and compare it with the theoretical values obtained: (1) assuming a terminal model; (2) using the calculated reactivity ratios; and (3) taking into account conversion. The results are illustrated in Table 7, which compares the various V-centred triad proportions corresponding to several copolymer samples at a given conversion. Relatively good agreement between experimental and theoretical data is observed in the low NAS composition range. Surprisingly, the simulated values at higher NAS contents,

particularly at the azeotropic composition, deviate significantly from the experimental ones; the presence of a proportion of AVV triads (with an average value of  $\sim 14\%$ ) is indeed found regardless of the conversion. This is not at all predicted by the simulation, which indicates a very small contribution (1%) of these triads. Such an effect is also shown above the azeotropic composition (as deduced from the V-centred triad distributions of samples COPO74).

It appears, then, that more NVP is incorporated into the copolymer chain than expected, the phenomenon being better evidenced when the NAS proportion is increased in the initial comonomer mixture. It is obvious that another  $r_{NVP}$  value should be used for predicting the contribution of such AVV triads; this is not valid when considering a terminal model for which one single pair of values should account for the monomer sequence distribution in the entire range of monomer feed composition. Such behaviour was not evidenced in the kinetic study, however it suggests that the regular set of propagation reactions should be modified. The occurrence of other reactions in addition to the classical scheme would result in a more complex copolymerization mechanism. Considering the chemical structure of NVP and NAS, two cases were investigated in more detail: complex participation<sup>20,21</sup> and the penultimate effect<sup>22,23</sup>.

#### Discussion on the copolymerization kinetic model

**Complex participation.** Transfer charge complexes can play a significant role in radical-initiated copolymerization when the two monomers are able to form donor–acceptor complexes<sup>24</sup>. For instance, Georgiev *et al.*<sup>20</sup> reported the role of transfer charge complexes during the polymerization of *N*-vinyl pyrrolidone and maleic anhydride. The tendency for this system towards alternation was found to be very high.

It is possible that the NVP–NAS system could give rise to such complexes. In the NVP molecule, the  $\pi$  electrons of the vinylic bond are conjugated with the  $\pi$  system of the amide group, which causes this double bond to be an electron donor, whereas NAS is electron-withdrawing in nature. Consequently, the existence of a transfer charge complex between NAS and NVP could be postulated (monomer/monomer or monomer/macroradical type).

It was attempted to find direct evidence for the formation of donor–acceptor complexes in the NVP–NAS binary system using <sup>13</sup>C n.m.r. Three different NVP/NAS molar ratios (1/1, 4/1 and 1/4) were used in the monomer feed mixture, at an overall concentration of 0.5 and 5 mol l<sup>-1</sup> in deuterated DMF, at room temperature. The position of all signals (C–C, C=O) of the different monomer mixtures was found to coincide with those of individual monomer solutions, indicating that the formation of complexes could be negligible under the selected experimental conditions.

**Table 7** Comparison of the experimental monomer sequence distribution (V-centred triads) with the theoretical one (based on knowledge of the reactivity ratios and conversion degree) (terminal, first-order Markov copolymerization)

Sample	$f_{A,0}$	Total molar conversion degree (%)	VVV	VVA + AVV	AVA
COPO10	0.10	10	0 (1)	15.6 (19)	84.4 (80)
COPO10	0.10	30	33.8 (30)	15.1 (23)	51.1 (47)
COPO48	0.50	90	0 (0)	14 (03)	86 (97)
COPO64	0.64	10	0 (0)	18 (01)	82 (99)
COPO64	0.64	80	0 (0)	11 (01)	89 (99)
COPO74	0.74	95	0 (0)	14 (01)	86 (99)

Values in parentheses indicate theoretical triad distribution using  $r_1 = 0.27$ ,  $r_2 = 0.01$ ;  $f_{A,0}$ : comonomer feed composition

**Table 8** Effect of experimental variables (reaction temperature, monomer concentration and nature of solvent) on the V-centred triad distribution

	DMF 60°C 0.5 mol l <sup>-1</sup>	DMF 30°C 0.5 mol l <sup>-1</sup>	DMF 60°C 0.07 mol l <sup>-1</sup>	DMF/AcOEt 60°C 0.5 mol l <sup>-1</sup>
VVV (%)	0	0	0	0
AVV + VVA (%)	18	14	13	13
AVA (%)	82	86	87	87

Moreover, considering that the formation of donor–acceptor complexes should be affected by temperature and dilution, the monomer sequence distribution of copolymers at the azeotropic composition was investigated by varying these two factors. One copolymerization was performed at 30°C instead of 60°C and another one at 0.07 mol l<sup>-1</sup> (overall concentration) instead of 0.5 mol l<sup>-1</sup>. The results of V-centred triads are reported in Table 8; it is clear that the monomer sequence distribution is not modified by either the reaction temperature or the monomer concentration.

These experiments seem to eliminate any significant participation of a charge transfer complex during NVP–NAS copolymerization, at least within the detection limit of the considered approach.

*Solvent effect.* We were limited as regards changing the polarity of the reaction solvent without altering the homogeneity of the medium during polymerization, since both monomers are quite different in nature. However, a copolymerization could be performed at the azeotropic composition in a mixture of ethyl acetate and dimethylformamide (1/1, v/v) in order to decrease significantly the solvent polarity. Pure ethyl acetate could not be used since the monomer mixture was found to precipitate. Again, as illustrated in Table 8, no marked effect was observed on the V-centred triad distribution.

As similarly shown by Nazarova *et al.*<sup>6</sup> for the same system, any clear evidence of interaction of NVP or NAS with the solvent could not be found.

*Penultimate effect.* The reactivity of a polymer radical with a given monomer can be affected by its penultimate group, especially when the terminal group is highly polar or bulky. Such effects have already been observed in the copolymerization of the following binary systems: styrene/acrylate, styrene/acrylonitrile and 4-maleimidobenzoic acid/methyl methacrylate<sup>22,23</sup>.

In the penultimate model, four reactivity ratios are defined instead of two in the terminal model:

$$r_1 = \frac{k_{111}}{k_{112}} \quad r'_1 = \frac{k_{211}}{k_{212}}$$

$$r_2 = \frac{k_{222}}{k_{221}} \quad r'_2 = \frac{k_{122}}{k_{121}}$$

where  $k_{hij}$  is the rate constant for the addition of a polymer radical terminated by monomer (*i*) whose penultimate group is monomer (*h*), to monomer (*j*).

It was considered that the reactivity ratio for the NAS-terminated radical is independent of its preceding unit due to its electron-deficient nature. On the contrary, a penultimate effect was assumed in the case of radicals terminated with the *N*-vinyl pyrrolidone monomer. When the NVP radical is neighboured by NAS, the latter would make the former electron deficient, increasing the radical's preference for the electron-rich NVP. In such a case, the ability of NVP to be included in the chain after an AV dyad is increased, thereby explaining the observation that a higher contribution of AVV triads was found than that theoretically predicted with the reactivity ratios  $r_1 = 0.27$  and  $r_2 = 0.01$ . Moreover, the higher the NAS proportion in the monomer mixture, the more important the tendency of NVP to be incorporated in the chain.

Using the experimental data, it was attempted to estimate the values of  $r_2$  and  $r'_2$  according to the method of Barson and Fenn<sup>25</sup>. Unfortunately, the corresponding plot did not exhibit any linear part, and no reliable values could be extrapolated. In addition, it was also found that any single set of reactivity ratios ( $r_1, r_2, r'_2$  or  $r_1, r'_1, r_2, r'_2$ ) could not give a good fit between theoretical predictions and V-centred triad distribution.

## CONCLUSIONS

Kinetics of the radical-initiated (co)polymerization of *N*-vinyl pyrrolidone (NVP) with *N*-acryloxy succinimide (NAS) in DMF were investigated allowing the reactivity ratios of the binary system to be calculated as  $r_{\text{NVP}} = 0.01 \pm 0.01$  and  $r_{\text{NAS}} = 0.27 \pm 0.04$ , assuming a terminal model;  $r_{\text{NVP}}$  was found to be very close to zero and poorly defined.

Since copolymer composition variation did not appear to be a suitable and sensitive tool to validate the kinetic model, the copolymer's microstructure was carefully investigated by <sup>13</sup>C n.m.r. spectroscopy. It was only possible to access the distribution of the NVP-centred triads, and all the copolymers were studied in order to compare the experimental distribution with the calculated one considering a terminal model. For NAS-poor comonomer feed compositions, calculated distribution and experimental ones seemed to be in good agreement. But for richer compositions (>40%), especially above the azeotropic composition (59 mol% NAS), the experimental values deviated significantly from the theoretical ones, and showed a contribution of AVV triads (average value of 14%) not at all predicted by the simulation (order of 1%).

This was a clear indication that the terminal model was not appropriate for describing the copolymerization of this system in the whole range of monomer composition. Unfortunately, any assumption concerning the occurrence of a more complicated kinetic model (penultimate effect or charge transfer complex participation, for instance) could not be confirmed experimentally. This does not mean that such a type of model (especially the possibility of complexation involving radical entities and monomer molecules) should be discarded and work is currently being carried out with a view to establish a more reliable model.

## REFERENCES

- 1 Arshady, R. *Adv. Polym. Sci.* 1994, **11**, 3
- 2 Monji, N. and Hoffman, A. S. *Appl. Biochem. Biotechnol.* 1987, **14**, 107
- 3 Yang, H. J., Cole, C. A., Monji, N. and Hoffman, A. S. *Polym. Chem., Part A* 1990, **38**, 219
- 4 Chen, J. P. and Hoffman, A. S. *Biomaterials* 1990, **11**, 631
- 5 Pollak, A., Blumenfeld, H., Wax, M., Baughn, R. L. and Whitesides, G. M. *J. Am. Chem. Soc.* 1980, **102**, 6324
- 6 Nazarova, O. V., Solovskij, M. V., Panarin, E. F., Denisov, V. M., Khachaturov, A. S., Koltsov, A. I. and Purkina, A. V. *Eur. Polym. J.* 1992, **28**(1), 97
- 7 Yamada, B., Kamei, B. H. and Otsu, T. *J. Polym. Sci.* 1980, **18**, 1917
- 8 Ganachaud, F. unpublished results
- 9 Kulkarni, M. G., Marhellkar, R. A. and Doraiswamy, L. K. *J. Polym. Sci., Polym. Lett. Edn* 1979, **17**, 713
- 10 Berger, K. C. and Meyerhoff, G. in 'Polymer Handbook', 3rd Edn (Eds J. Brandrup and E. H. Immergut), Wiley Interscience, New York, 1989



- 11 De Abajo, J., Madruga, E. L., San Roman, J., De la Campa, J. G. and Guzman, J. *Polymer* 1987, **27**, 889
- 12 Fineman, M. and Ross, D. *J. Polym. Sci.* 1950, **5**, 529
- 13 Kelen, T. and Tüdös, F. *J. Macromol. Sci., Chem. A*, 1975, **9**, 1
- 14 Tidwell, P. W. and Mortimer, G. A. *J. Polym. Sci., Part A* 1965, **3**, 369
- 15 Reddy, B. S. R., Arshady, R. and George, M. H. *Eur. Polym. J.* 1985, **21**(6), 511
- 16 Soundarajan, S. and Reddy, B. S. R. *Polymer* 1993, **34**(10), 2224
- 17 Wen, S., Xiaonan, Y. and Stevenson, W. T. K. *Polym. Int.* 1992, **27**, 81
- 18 Llauro, M. F., Pichot, C., Guillot, J., Rios, L., Cruz, M. A. and Guzman, C., *Polymer* 1987, **27**, 889
- 19 Bovey, F. in 'Chain Microstructure and Conformation of Macromolecules', Academic Press, New York, 1982
- 20 Georgiev, G., Konstantinov, C. and Kabaivanov, V. *Macromolecules* 1992, **25**, 6302
- 21 Beaune, O., Bessiere, J.-M. and Boutevin, B. *Eur. Polym. J.* 1992, **28**(12), 1501
- 22 Fukuda, T., Ma, Y. D. and Inagaki, H. *Polym. J.* 1982, **14**, 705
- 23 Nair, C. P. R. *Macromolecules* 1993, **26**, 47
- 24 Mulliken, R. S. and Person, W. B. in 'Molecular Complexes', Wiley Interscience, New York, 1969
- 25 Barson, C. A. and Fenn, D. R. *Eur. Polym. J.* 1985, **23**, 833